ELSEVIER

Chemical Physics 259 (2000) 11–26

Chemical Physics

www.elsevier.nl/locate/chemphys

A recursive Kohn variational algorithm for the Green's operator: application to the T-matrix

David Brown *

Department of Applied Physics, Columbia University and the Goddard Institute for Space Studies, New York, NY 10025, USA

Received 13 September 1999

Abstract

A recursive version of the Kohn variational principle for the Green's operator is presented. An expression for the off-shell T-matrix is derived which is valid in the presence of a hard wall potential and which is conveniently evaluated using the recursive algorithm. The off-shell T-matrix elements for scattering systems with and without hard wall components to the potential are computed using this algorithm.

1. Introduction

For an isolated collision at a given energy, the most complete physical description consists of the probabilities of all possible transitions between quantum states of the colliding particles before and after the collision. This information is contained in the on-shell matrix elements of the T-operator. The term "on-shell" means that the matrix elements are evaluated between states of the same energy (and at the same energy at which the intrinsically energy-dependent T-operator is evaluated). This condition merely reflects the conservation of energy in the absence of an external field. It is often asserted that only the on-shell T-matrix elements have physical significance or correspond to observable results [1]. It is nevertheless possible to calculate *off*-shell matrix elements of the T-operator between states of different energies.

When an electromagnetic field is present, a collision can result in transitions between states of different energies. In such cases, approximate methods involving field-free T-matrix operators are sometimes used to compute the transition probabilities. An example is the Kroll–Watson approximation for charged particle collisions in the presence of a low-frequency laser field, which expresses the scattering probabilities in terms of on-shell field free cross sections [2]. The electron–atom scattering experiments of Wallbank and Holmes [3–5] showed the limitations of this approximation. Subsequent theoretical studies showed that the Kroll–Watson approximation could be improved if off-shell T-matrix information was included [6,7].

Another example in which off-shell information can be used arises in the theory of spectral lineshapes. Several Liouville space formalisms have been derived for the shape of an absorption or emission line as a function of frequency [8–10].

* Present address: 221, Degraw St. 2, Brooklyn, NY 11231, USA.

E-mail address: dbrownx@aol.com (D. Brown).

0301-0104/00/$ - see front matter
PII: S0301-0104(00)00151-8

Fano's derivation for lineshapes under conditions in which the absorbing or emitting particle undergoes binary collisions with other particles (the binary collision approximation) is the most relevant to this discussion. Fano's expression is extremely complicated and involves off-shell T-matrix elements for the colliding particles in the absence of a field. When the electric field is tuned to near the resonant frequency of absorption or emission (with "near" being a somewhat subjective concept), Fano's expression simplifies to one involving only on-shell T-matrix quantities; this is the impact approximation, so-called because the duration of the collision is assumed to be much less than the time between collisions. The impact approximation has been widely and successfully used in lineshape studies, but recent experiments on the H_2S–He collision system have suggested that this approximation may not be appropriate under some experimental conditions [11]. In order to test the impact approximation, we require the ability to compute off-shell T-matrix elements.

Even in the absence of an external field, the off-shell T-matrix is employed in approximate methods, such as multiple scattering expansions [12] and the impulse approximation [13], for systems too large or complicated to treat exactly. The off-shell T-matrix has recently appeared in studies of atom–diatom [25,14], atom–surface [15], molecule–surface [16], and charge transfer [17] scattering systems, and has been used to extend the range of accuracy of the fixed-nuclei approximation for electron–molecule scattering at low energies [18,19].

Several theoretical studies have been devoted to the off-shell T-matrix [20–31]; it has been computed analytically for a handful of simple 1-D potentials such as hard walls [24] and square wells [31], and semiclassical [28,30] and variational approaches [32] have been derived as well. Unfortunately, the utility of the off-shell T-matrix is limited by the fact that practical algorithms for its computation have been presented only for 1-D systems. For lineshape studies in particular, it is important that off-shell T-matrix elements be computed for more complicated potentials. In this paper a technique is presented which can compute the off-shell T-matrix for more general systems.

The algorithm developed in this paper is based on the Kohn variational principle for the Green's operator presented by Miller and Jansen op de Haar [33]. The difficulty with variational approaches is that as the dimensionality of the problem increases the basis size can become extremely large. To circumvent this problem, we divide configuration space into cells, derive a recursion relation for the coefficients of the variational solution in one cell in terms of the coefficients in the surrounding cells, and recombine them to evaluate the variational functional, which is a matrix element of the Green's operator. In Section 2, we will describe the recursion relation for a simple 1-D problem and discuss the relation of the technique to the off-shell T-matrix. In Section 3, computational details for the trial problems are given. In Section 4, off-shell T-matrix results for a 1-D Lennard-Jones potential and a model rotationally inelastic atom–diatom problem are presented, and Section 5 concludes.

2. Theory

We first discuss the recursive Kohn variational principle method for Green's operator matrix elements in general. We then apply it to the computation of off-shell T-matrix elements for systems with or without a hard wall potential.

2.1. Recursive KVP

For concreteness we discuss the case of 1-D scattering of a point particle with reduced mass μ in a spherically symmetric potential. At the end of this section we will touch briefly on the straightforward generalization to more complicated systems. We have a Hamiltonian

$$H = -\frac{\hbar^2}{2\mu}\left(\frac{\mathrm{d}^2}{\mathrm{d}r^2} - \frac{l(l+1)}{r^2}\right) + V(r) \tag{1}$$

and seek to compute the matrix elements

$$\langle f|G^+(E)|g\rangle = \lim_{\epsilon\to\infty} \int_a^\infty \mathrm{d}r \int_a^\infty \mathrm{d}r' f(r) \times \langle r|(E - H + \mathrm{i}\epsilon)^{-1}|r'\rangle g(r'), \tag{2}$$

where a may or may not be zero, between $\mathscr{L}^2$ functions f and g. Miller and Jansen op de Haar [33] noted that the functional

$$I[\chi,\tilde{\chi}] = \langle\tilde{\chi}|g\rangle + \langle f|\chi\rangle + \langle\tilde{\chi}|H-E|\chi\rangle \tag{3}$$

is stationary to second order about the desired matrix element as long as the basis for χ and $\tilde{\chi}$ behaves only as an outgoing plane wave at infinite r, which enforces the $+i\epsilon$ boundary condition. Note that in the matrix element (3) the function $f(r)$ appears in the integrand rather than its complex conjugate. This definition of the inner product is a common practice and will apply throughout the paper [33].

We assume that $f(r)$, $g(r)$ and $V(r)$ are all negligible for $r \geqslant r_{\max}$, then divide the range $[a, r_{\max}]$ into N sectors (which need not be equal in size) defined by the N coordinate values $r = r_i$, with $r_N = r_{\max}$. Next we choose bases $\{\phi_n^i, n = 1,\ldots,n_i\}$ on each sector. For convenience we take these functions to be real and orthonormal, but neither restriction is necessary. We assume that the functions ϕ_n^1 obey some suitable boundary condition at $r = a$ (typically $\phi_n^1(a) = 0$ for all n). It is important, as in the cellular R- or log-derivative matrix algorithm, that the functions ϕ_n^i do not otherwise obey any fixed boundary condition at $r = r_i$ or $r = r_{i+1}$ [34]. Finally, we take the range $(r_{\max},\infty)$ to be the $(N+1)$th sector and let $\phi_1^{N+1}(r) = h_l^+(kr)$, which is the outgoing Ricatti–Hankel function with $k = \sqrt{2\mu E}/\hbar$.

We expand χ and $\tilde{\chi}$ in this basis

$$\chi = \sum_{i=1}^{N+1}\sum_{n=1}^{n_i} c_n^i \phi_n^i(r), \tag{4}$$

$$\tilde{\chi} = \sum_{i=1}^{N+1}\sum_{n=1}^{n_i} d_n^i \phi_n^i(r). \tag{5}$$

We can construct Hamiltonian matrix elements on the range $[a, r_{\max}]$

$$\langle\phi_m^i|H|\phi_n^j\rangle = \langle\phi_m^i|H|\phi_n^i\rangle\delta_{ij} = \mathbf{H}_{mn}^i\delta_{ij}. \tag{6}$$

Since the sector bases obey no fixed boundary conditions at the boundaries between sectors, the Hamiltonian matrices on each sector are asymmetric,

$$\mathbf{H}_{mn}^i = \mathbf{H}_{nm}^i - \frac{\hbar^2}{2\mu}\Big[\phi_m^i(r_{i+1})\phi_n^{i'}(r_{i+1}) - \phi_n^i(r_{i+1})\phi_m^{i'}(r_{i+1}) - \phi_m^i(r_i)\phi_n^{i'}(r_i) + \phi_n^i(r_i)\phi_m^{i'}(r_i)\Big], \tag{7}$$

where the prime denotes differentiation with respect to r. We can write in matrix form

$$\mathbf{H}^i = \mathbf{H}_{\mathrm{S}}^i + \mathbf{U}_l^i\mathbf{W}_l\mathbf{U}_l^{i\mathrm{T}} + \mathbf{U}_r^i\mathbf{W}_r\mathbf{U}_r^{i\mathrm{T}} \quad (2 \leqslant i \leqslant N), \tag{8}$$

where $\mathbf{H}_{\mathrm{S}}^i$ is the symmetric part of $\mathbf{H}^i$,

$$\mathbf{W}_l = -\mathbf{W}_r = \begin{pmatrix} 0 & -\frac{\hbar^2}{4\mu} \\ \frac{\hbar^2}{4\mu} & 0 \end{pmatrix} \tag{9}$$

and $\mathbf{U}_l^i$ and $\mathbf{U}_r^i$ are $n_i \times 2$ matrices with elements

$$\left[\mathbf{U}_l^i\right]_{n1} = \phi_n^i(r_i), \tag{10}$$

$$\left[\mathbf{U}_l^i\right]_{n2} = \frac{\mathrm{d}}{\mathrm{d}r}\phi_n^i(r_i), \tag{11}$$

$$\left[\mathbf{U}_r^i\right]_{n1} = \phi_n^i(r_{i+1}), \tag{12}$$

$$\left[\mathbf{U}_r^i\right]_{n2} = \frac{\mathrm{d}}{\mathrm{d}r}\phi_n^i(r_{i+1}). \tag{13}$$

For sector 1 the second term on the right-hand side of Eq. (8) is absent, since the functions ϕ_n^1 obey fixed boundary conditions at $r = a$. On each sector we also require the $n_i \times 1$ vectors whose elements are

$$[\mathbf{f}_i]_n = \langle\phi_n^i|f\rangle, \tag{14}$$

$$[\mathbf{g}_i]_n = \langle\phi_n^i|g\rangle, \tag{15}$$

$$[\mathbf{c}_i]_n = c_n^i, \tag{16}$$

$$[\mathbf{d}_i]_n = d_n^i. \tag{17}$$

We now insert the expression (5) into Eq. (3) and impose the requirements of continuity and differentiability of χ and $\tilde{\chi}$ as constraints on I. We have, in matrix form

$$I = \sum_{i=1}^{N}\Big\{\mathbf{f}_i^{\mathrm{T}}\mathbf{c}_i + \mathbf{d}_i^{\mathrm{T}}\mathbf{g}_i + \mathbf{d}_i^{\mathrm{T}}(\mathbf{H}^i - E\mathbf{1})\mathbf{c}_i + \mathbf{\Lambda}_c^{i\mathrm{T}}(\mathbf{U}_r^{i\mathrm{T}}\mathbf{c}_i - \mathbf{U}_l^{i+1\mathrm{T}}\mathbf{c}_{i+1}) + (\mathbf{d}_i^{\mathrm{T}}\mathbf{U}_r^i - \mathbf{d}_{i+1}^{\mathrm{T}}\mathbf{U}_l^{i+1})\mathbf{\Lambda}_d^i\Big\}, \tag{18}$$

where $\mathbf{\Lambda}_c^i$ is the 2×1 vector of Lagrange multipliers corresponding to the constraints of continuity and differentiability of χ at $r = r_i$ while $\mathbf{\Lambda}_d^i$ is its analog for $\tilde{\chi}$. Inspection of Eq. (18) shows that differentiation with respect to $\mathbf{d}_i^{\mathrm{T}}$ and $\mathbf{\Lambda}_c^{i^{\mathrm{T}}}$ yields coupled linear equations for $\mathbf{c}_i$, $\mathbf{c}_{i+1}$, and $\mathbf{\Lambda}_d^i$, while differentiation with respect to $\mathbf{c}_i$ and $\mathbf{\Lambda}_d^i$ yields equations for $\mathbf{d}_i^{\mathrm{T}}$, $\mathbf{d}_{i+1}^{\mathrm{T}}$, and $\mathbf{\Lambda}_c^{i^{\mathrm{T}}}$. We now turn to the solution of these equations.

2.1.1. Solution for the coefficients on the first sector

After differentiating Eq. (18) with respect to $\mathbf{d}_i^{\mathrm{T}}$ and $\mathbf{\Lambda}_c^{i^{\mathrm{T}}}$ and setting these derivatives equal to zero, we arrive at the following linear equation for $\mathbf{c}_1$:

$$[\mathbf{a}_1(E) + \mathbf{U}_r^1 \mathbf{W}_r \mathbf{U}_r^{1^{\mathrm{T}}}]\mathbf{c}_1 = -\mathbf{g}_1 - \mathbf{U}_r^1 \mathbf{\Lambda}_d^1 \tag{19}$$

or

$$\mathbf{a}_1(E)\mathbf{c}_1 = -\mathbf{g}_1 - \mathbf{U}_r^1 \tilde{\mathbf{\Lambda}}_d^1, \tag{20}$$

where $\mathbf{a}_1$ is the symmetric matrix

$$\mathbf{a}_1(E) = \mathbf{H}_{\mathrm{S}}^1 - E\mathbf{1} \tag{21}$$

and

$$\tilde{\mathbf{\Lambda}}_d^1 = \mathbf{\Lambda}_d^1 + \mathbf{W}_r \mathbf{U}_r^{1^{\mathrm{T}}} \mathbf{c}_1. \tag{22}$$

(We suppress the energy argument from now on.) Eq. (20) has the solution

$$\mathbf{c}_1 = -\mathbf{a}_1^{-1}\mathbf{g}_1 - \mathbf{a}_1^{-1}\mathbf{U}_r^1 \tilde{\mathbf{\Lambda}}_d^1. \tag{23}$$

We use the conditions that the solution be continuous and differentiable at $r = r_1$ – in matrix form, $\mathbf{U}_r^{1^{\mathrm{T}}}\mathbf{c}_1 = \mathbf{U}_l^{2^{\mathrm{T}}}\mathbf{c}_2$ – to eliminate $\tilde{\mathbf{\Lambda}}_d^1$ in favor of $\mathbf{c}_1$ and $\mathbf{c}_2$. This leads to the recursion relation

$$\begin{aligned}\mathbf{c}_1 = {} & -\mathbf{a}_1^{-1}\left(\mathbf{1} - \mathbf{U}_r^1 \mathbf{x}_1^{-1} \mathbf{U}_r^{1^{\mathrm{T}}} \mathbf{a}_1^{-1}\right)\mathbf{g}_1 \\ & + \mathbf{a}_1^{-1}\mathbf{U}_r^1 \mathbf{x}_1^{-1} \mathbf{U}_l^{2^{\mathrm{T}}} \mathbf{c}_2,\end{aligned} \tag{24}$$

$$\mathbf{c}_1 = \mathbf{c}_1^0 + \mathbf{a}_1^{-1}\mathbf{U}_r^1 \mathbf{x}_1^{-1} \mathbf{U}_l^{2^{\mathrm{T}}} \mathbf{c}_2, \tag{25}$$

where $\mathbf{x}_1 = \mathbf{U}_r^{1^{\mathrm{T}}} \mathbf{a}_1^{-1} \mathbf{U}_r^1$. Note that

$$\mathbf{U}_r^{1^{\mathrm{T}}} \mathbf{c}_1^0 = \begin{pmatrix} 0 \\ 0 \end{pmatrix} \quad \text{and} \quad \mathbf{U}_r^{1^{\mathrm{T}}} \mathbf{c}_1 = \mathbf{U}_l^{2^{\mathrm{T}}} \mathbf{c}_2,$$

so that the constraints are satisfied.

Similarly, differentiating Eq. (18) with respect to $\mathbf{c}_1$ and $\mathbf{\Lambda}_d^1$ yields

$$\begin{aligned}\mathbf{d}_1^{\mathrm{T}} = {} & -\mathbf{f}_1^{\mathrm{T}}\left(\mathbf{1} - \mathbf{a}_1^{-1}\mathbf{U}_r^1 \mathbf{x}_1^{-1} \mathbf{U}_r^{1^{\mathrm{T}}}\right)\mathbf{a}_1^{-1} \\ & + \mathbf{d}_2^{\mathrm{T}}\mathbf{U}_l^2 \mathbf{x}_1^{-1} \mathbf{U}_r^{1^{\mathrm{T}}} \mathbf{a}_1^{-1},\end{aligned} \tag{26}$$

$$\mathbf{d}_1^{\mathrm{T}} = \mathbf{d}_1^{0^{\mathrm{T}}} + \mathbf{d}_2^{\mathrm{T}}\mathbf{U}_l^2 \mathbf{x}_1^{-1} \mathbf{U}_r^{1^{\mathrm{T}}} \mathbf{a}_1^{-1}. \tag{27}$$

2.1.2. Solutions for the coefficients on intermediate sectors

Next, we differentiate with respect to $\mathbf{d}_2^{\mathrm{T}}$ and $\mathbf{\Lambda}_c^{2^{\mathrm{T}}}$. Now we have

$$\begin{aligned}&[\mathbf{a}_2 + \mathbf{U}_l^2 \mathbf{W}_l \mathbf{U}_l^{2^{\mathrm{T}}} + \mathbf{U}_r^2 \mathbf{W}_r \mathbf{U}_r^{2^{\mathrm{T}}}]\mathbf{c}_2 \\ &\quad = -\mathbf{g}_2 + \mathbf{U}_l^2 \mathbf{\Lambda}_d^1 - \mathbf{U}_r^2 \mathbf{\Lambda}_d^2\end{aligned} \tag{28}$$

or

$$\mathbf{a}_2\mathbf{c}_2 = -\mathbf{g}_2 + \mathbf{U}_l^2 \tilde{\mathbf{\Lambda}}_d^1 - \mathbf{U}_r^2 \tilde{\mathbf{\Lambda}}_d^2, \tag{29}$$

where it is easily shown that the vector $\tilde{\mathbf{\Lambda}}_d^1$ is the same as that from the previous section, and

$$\mathbf{a}_2 = \mathbf{H}_{\mathrm{S}}^2 - E\mathbf{1}. \tag{30}$$

Plugging the solutions to Eq. (19) into Eq. (29) yields the modified equation

$$\tilde{\mathbf{a}}_2\mathbf{c}^2 = -\tilde{\mathbf{g}}_2 - \mathbf{U}_r^2 \tilde{\mathbf{\Lambda}}_d^2, \tag{31}$$

where

$$\tilde{\mathbf{a}}_2 = \mathbf{a}_2 + \mathbf{U}_l^2 \mathbf{x}_1^{-1} \mathbf{U}_l^{2^{\mathrm{T}}} \tag{32}$$

and

$$\tilde{\mathbf{g}}_2 = \mathbf{g}_2 + \mathbf{U}_l^2 \mathbf{x}_1^{-1} \mathbf{U}_r^{1^{\mathrm{T}}} \mathbf{a}_1^{-1} \mathbf{g}_1. \tag{33}$$

Eq. (31) is formally identical to Eq. (20), and its solution in terms of the coefficients $\mathbf{c}_3$ proceeds exactly as did the solution of Eq. (20) for $\mathbf{c}_1$. Thus,

$$\begin{aligned}\mathbf{c}_2 = {} & -\tilde{\mathbf{a}}_2^{-1}\left(\mathbf{1} - \mathbf{U}_r^2 \mathbf{x}_2^{-1} \mathbf{U}_r^{2^{\mathrm{T}}} \tilde{\mathbf{a}}_2^{-1}\right)\tilde{\mathbf{g}}_2 \\ & + \tilde{\mathbf{a}}_2^{-1}\mathbf{U}_r^2 \mathbf{x}_2^{-1} \mathbf{U}_l^{3^{\mathrm{T}}} \mathbf{c}^3 \\ = {} & \mathbf{c}_2^0 + \tilde{\mathbf{a}}_2^{-1}\mathbf{U}_r^2 \mathbf{x}_2^{-1} \mathbf{U}_l^{3^{\mathrm{T}}} \mathbf{c}^3,\end{aligned} \tag{34}$$

where now

$$\mathbf{x}_2 = \mathbf{U}_r^{2^{\mathrm{T}}} \tilde{\mathbf{a}}_2^{-1} \mathbf{U}_r^2. \tag{35}$$

As before, $\mathbf{U}_r^{2^{\mathrm{T}}} \mathbf{c}_0^2 = 0$. Again, $\mathbf{d}_2$ obeys an equation analogous to the transpose of Eq. (34) with $\mathbf{d}_3$ in place of $\mathbf{c}_3$, $\tilde{\mathbf{f}}_2$ replacing $\tilde{\mathbf{g}}_2$, and $\tilde{\mathbf{f}}_2$ de-

fined by Eq. (33) with $\mathbf{f}_2$ replacing $\mathbf{g}_2$. This treatment applies to all sectors $2 \leqslant i \leqslant N$. For $\mathbf{c}_i$, we have

$$\begin{aligned}\mathbf{c}_i &= -\tilde{\mathbf{a}}_i^{-1}\left(\mathbf{1} - \mathbf{U}_r^i \mathbf{x}_i^{-1} \mathbf{U}_r^{i^{\mathrm{T}}} \tilde{\mathbf{a}}_i^{-1}\right)\tilde{\mathbf{g}}_i \\ &\quad + \tilde{\mathbf{a}}_i^{-1}\mathbf{U}_r^i \mathbf{x}_i^{-1}\mathbf{U}_l^{(i+1)^{\mathrm{T}}}\mathbf{c}_{i+1} \\ &= \mathbf{c}_i^0 + \tilde{\mathbf{a}}_i^{-1}\mathbf{U}_r^i \mathbf{x}_i^{-1}\mathbf{U}_l^{(i+1)^{\mathrm{T}}}\mathbf{c}_{i+1} \end{aligned} \tag{36}$$

with

$$\tilde{\mathbf{a}}_i = \left(\mathbf{H}_{\mathrm{S}}^i - E\mathbf{1}\right) + \mathbf{U}_l^i \mathbf{x}_{i-1}^{-1}\mathbf{U}_l^{i^{\mathrm{T}}}, \tag{37}$$

$$\mathbf{x}_i = \mathbf{U}_r^{i^{\mathrm{T}}}\tilde{\mathbf{a}}_i^{-1}\mathbf{U}_r^i \tag{38}$$

and

$$\tilde{\mathbf{g}}_i = \mathbf{g}_i + \mathbf{U}_l^i \mathbf{x}_{i-1}^{-1}\mathbf{U}_r^{(i-1)^{\mathrm{T}}}\tilde{\mathbf{a}}_{i-1}^{-1}\tilde{\mathbf{g}}_{i-1}. \tag{39}$$

Corresponding equations and definitions apply to the solutions for $\mathbf{d}_i$.

2.1.3. Solution for the coefficients on the Nth sector

On the Nth sector, we have

$$\tilde{\mathbf{a}}_N \mathbf{c}_N = -\tilde{\mathbf{g}}_N - \mathbf{U}_r^N \tilde{\mathbf{\Lambda}}_d^N. \tag{40}$$

Because f, g and the potential are negligible at $r = r_{\max}$, and since $h_l^+(kr)$ is an eigenfunction with energy E for $r \geqslant r_{\max}$, the basis set expansion on the $(N+1)$th sector contributes to the functional *only through the constraints*. This fact is reflected in the fact that the summation over sectors in Eq. (18) extends only to N rather than $N+1$, and that only in the constraint terms do the coefficients c_1^{N+1} and d_1^{N+1} appear.

For notational convenience, we define the 2×1 vector $\mathbf{q}$ as

$$\mathbf{q} = \mathbf{U}_l^{N+1^{\mathrm{T}}} = \begin{pmatrix} h_l^+(kr_{\max}) \\ \frac{\mathrm{d}h_l^+}{\mathrm{d}r}(kr_{\max}) \end{pmatrix}. \tag{41}$$

Differentiating Eq. (18) with respect to d_1^{N+1} and setting the result equal to zero yields

$$\mathbf{U}_l^{N+1}\mathbf{\Lambda}_d^N = \mathbf{q}^{\mathrm{T}}\mathbf{\Lambda}_d^N = 0. \tag{42}$$

Recall that

$$\begin{aligned}\tilde{\mathbf{\Lambda}}_d^N &= \mathbf{\Lambda}_d^N + \mathbf{W}_r \mathbf{U}_r^{N^{\mathrm{T}}}\mathbf{c}_N, & (43)\\ &= \mathbf{\Lambda}_d^N - \mathbf{W}_l \mathbf{q} c_1^{N+1}. & (44)\end{aligned}$$

Since $\mathbf{W}_l$ is antisymmetric, we have

$$\mathbf{q}^{\mathrm{T}}\tilde{\mathbf{\Lambda}}_d^N = 0; \tag{45}$$

that is, $\tilde{\mathbf{\Lambda}}_d^N$ and $\mathbf{\Lambda}_d^N$ satisfy the same equation.

We now use the constraint (45) to solve for c_1^{N+1},

$$c_1^{N+1} = -(\mathbf{q}^{\mathrm{T}}\mathbf{x}_N^{-1}\mathbf{q})^{-1}\mathbf{q}^{\mathrm{T}}\mathbf{x}_N^{-1}\mathbf{U}_r^{N^{\mathrm{T}}}\tilde{\mathbf{a}}_N^{-1}\tilde{\mathbf{g}}_N \tag{46}$$

which gives

$$\begin{aligned}\mathbf{c}_N &= -\tilde{\mathbf{a}}_N^{-1}\left(\mathbf{1} - \mathbf{U}_r^N \mathbf{x}_N^{-1}\mathbf{U}_r^{N^{\mathrm{T}}}\tilde{\mathbf{a}}_N^{-1}\right)\tilde{\mathbf{g}}_N \\ &\quad - \tilde{\mathbf{a}}_N^{-1}\mathbf{U}_r^N \mathbf{x}_N^{-1}\mathbf{q}(\mathbf{q}^{\mathrm{T}}\mathbf{x}_N^{-1}\mathbf{q})^{-1}\mathbf{q}^{\mathrm{T}}\mathbf{x}_N^{-1}\mathbf{U}_r^{N^{\mathrm{T}}}\tilde{\mathbf{a}}_N^{-1}\tilde{\mathbf{g}}_N, \end{aligned} \tag{47}$$

$$\mathbf{c}_N = \mathbf{c}_N^0 + \mathbf{c}_N^g, \tag{48}$$

where evidently all the effects of the asymptotic behavior of the Green's operator are contained in $\mathbf{c}_N^g$.

An analogous procedure for $\mathbf{d}_N^{\mathrm{T}}$ gives

$$\begin{aligned}\mathbf{d}_N^{\mathrm{T}} &= -\tilde{\mathbf{f}}_N^{\mathrm{T}}\left(\mathbf{1} - \tilde{\mathbf{a}}_N^{-1}\mathbf{U}_r^N \mathbf{x}_N^{-1}\mathbf{U}_r^{N^{\mathrm{T}}}\right)\tilde{\mathbf{a}}_N^{-1} \\ &\quad - \tilde{\mathbf{f}}_N^{\mathrm{T}}\tilde{\mathbf{a}}_N^{-1}\mathbf{U}_r^N \mathbf{x}_N^{-1}\mathbf{q}(\mathbf{q}^{\mathrm{T}}\mathbf{x}_N^{-1}\mathbf{q})^{-1}\mathbf{q}^{\mathrm{T}}\mathbf{x}_N^{-1}\mathbf{U}_r^{N^{\mathrm{T}}}\tilde{\mathbf{a}}_N^{-1}, \end{aligned} \tag{49}$$

$$\mathbf{d}_N^{\mathrm{T}} = \mathbf{d}_N^{0^{\mathrm{T}}} + \mathbf{d}_N^{g^{\mathrm{T}}}. \tag{50}$$

2.1.4. Assembling the matrix element

The last step in the evaluation of the Green's operator matrix element is the substitution of the solutions $\mathbf{c}_i$ and $\mathbf{d}_i^{\mathrm{T}}$ into Eq. (18). Mercifully, we do not need to evaluate all these coefficients explicitly; we only require $\mathbf{c}_i^0$, $\mathbf{d}_i^{0^{\mathrm{T}}}$, $\mathbf{c}_N^g$ and $\mathbf{d}_N^{g^{\mathrm{T}}}$. This exercise is straightforward but tedious, so I will give the results followed by a few comments which may help the interested or cautious reader to verify them.

The final result is

$$\langle f|G^+(E)|g\rangle = I = \sum_{i=0}^{N} I_i^0 + I_N^g, \tag{51}$$

where

$$I_i^0 = -\tilde{\mathbf{f}}_i^{\mathrm{T}}\tilde{\mathbf{a}}_i^{-1}\tilde{\mathbf{g}}_i + \tilde{\mathbf{f}}_i^{\mathrm{T}}\tilde{\mathbf{a}}_i^{-1}\mathbf{U}_r^i\mathbf{x}_i^{-1}\mathbf{U}_r^{i^{\mathrm{T}}}\tilde{\mathbf{a}}_i^{-1}\tilde{\mathbf{g}}_i \tag{52}$$

in which, by definition, $\tilde{\mathbf{f}}_1 = \mathbf{f}_1$, $\tilde{\mathbf{g}}_1 = \mathbf{g}_1$ and $\tilde{\mathbf{a}}_1 = \mathbf{a}_1$. Also,

$$I_N^g = -\tilde{\mathbf{f}}_N^{\mathrm{T}}\tilde{\mathbf{a}}_N^{-1}\mathbf{U}_r^N\mathbf{q}(\mathbf{q}^{\mathrm{T}}\mathbf{x}_N^{-1}\mathbf{q})^{-1}\mathbf{q}^{\mathrm{T}}\mathbf{U}_r^{N^{\mathrm{T}}}\tilde{\mathbf{a}}_N^{-1}\tilde{\mathbf{g}}_N. \tag{53}$$

For each sector i, the contributions to the functional from previous sectors add to effectively replace $\mathbf{f}_i$, $\mathbf{g}_i$, and $\mathbf{a}_i$ with $\tilde{\mathbf{f}}_i$, $\tilde{\mathbf{g}}_i$, and $\tilde{\mathbf{a}}_i$, respectively. Although in Eq. (18) the full sector Hamiltonians must be used, it turns out that *all* contributions to the total functional due to the anti-Hermitian parts of the Hamiltonians cancel. To show this, one uses the facts that

$$\mathbf{U}_r^{i^{\mathrm{T}}}\mathbf{c}_i^0 = \mathbf{U}_r^{i^{\mathrm{T}}}\mathbf{d}_i^0 = \begin{pmatrix} 0 \\ 0 \end{pmatrix}$$

and that $\mathbf{W}_r = -\mathbf{W}_l$.

2.1.5. Multichannel Green's operator elements

Extension to multiple dimensions is straightforward. One divides configuration space into cells. On the boundaries of each cells, surface bases are constructed. The constraints of continuity of χ, $\tilde{\chi}$, and their normal derivatives across the boundaries are imposed on each component of χ and $\tilde{\chi}$ in the surface basis. Thus, for example, the vectors $\mathbf{\Lambda}_{c,d}^i$ will have dimension $2n_{\mathrm{s}} \times 1$ and $\mathbf{x}_i$ has dimension $2n_{\mathrm{s}} \times 2n_{\mathrm{s}}$, where n_{s} is the number of surface functions on which the continuity and differentiability conditions are being imposed in the ith sector.

As an example, consider the atom-rigid rotor scattering problem, which will be treated in more detail in the next section. The coordinates are R, the distance between the atom and the center of mass of the rigid rotor, and the spherical polar coordinates for the atom and the rigid rotor. We divide R into N sectors; thus, the "boundary surface" for the ith cell consists of the radial values R_{i-1} and R_i. For each value of R_i, we define a basis in the remaining coordinates, and the differentiability and continuity of χ and $\tilde{\chi}$ across $R = R_i$ is imposed separately on each component. The resulting recursion equations have a form identical to those for the 1-D situation, except that $\mathbf{U}_l^i$ has dimension $n_i \times 2n_{\mathrm{s}}^{i-1}$, $\mathbf{U}_r^i$ has dimension $n_i \times 2n_{\mathrm{s}}^i$, and $\mathbf{x}_i$ has dimension $2n_{\mathrm{s}}^i \times 2n_{\mathrm{s}}^i$, where as before n_i is the size of the sector basis and n_{s}^i is the size of the surface basis at $R = R_i$.

2.2. Off-shell T-matrix in the presence of a hard wall

When no hard wall is present, the T-matrix can be written in terms of the Green's operator as

$$\mathbf{T} = \mathbf{V} + \mathbf{V}\mathbf{G}^+(E)\mathbf{V}. \tag{54}$$

To compute matrix elements of the form $\langle \mathbf{k}_{\mathrm{f}}|T(E)|\mathbf{k}_{\mathrm{i}}\rangle$, we would substitute $f(\mathbf{r}) = V(\mathbf{r}) \times \exp(\mathrm{i}\mathbf{k}_{\mathrm{f}} \cdot \mathbf{r})/(2\pi)^{3/2}$ and $g(\mathbf{r}) = V(\mathbf{r})\exp(\mathrm{i}\mathbf{k}_{\mathrm{i}} \cdot \mathbf{r})/(2\pi)^{3/2}$ into Eq. (3). When the potential has a hard wall contribution so that it is formally infinite within the region bounded by the wall, expression (54) may be problematic.

Here we briefly review the off-shell T-matrix and develop an expression for the T-matrix element that is valid when a hard wall is present and reduces to Eq. (54) when it is not. The treatment herein is based on that of Laughlin and Scott [24]. Let us write the Hamiltonian $\mathbf{H}$ as $\mathbf{H} = \mathbf{H}_0 + \mathbf{V}$ and define eigenstates $\phi_{\mathrm{i,f}}^0$ of $\mathbf{H}_0$ such that

$$\mathbf{H}_0\phi_{\mathrm{i,f}}^0 = E_{\mathrm{i,f}}\phi_{\mathrm{i,f}}^0, \tag{55}$$

where $E_{\mathrm{i,f}}$ is energy of the initial or final state. These energies need not be equal, or equal to the energy E at which the Green's operator is evaluated. For our 1-D example, $\mathbf{H}_0$ would be the 1-D kinetic energy operator and $\phi_{\mathrm{i,f}}^0 = a_{\mathrm{i,f}}j_l(k_{\mathrm{i,f}}r)$, where j_l is the Ricatti–Bessel function and $a_{\mathrm{i,f}}$ are suitable normalization constants. We seek

$$\langle \phi_{\mathrm{f}}^0|\mathbf{T}(E)|\phi_{\mathrm{i}}^0\rangle = \langle \phi_{\mathrm{f}}^0|\mathbf{V}\Omega^+(E)|\phi_{\mathrm{i}}^0\rangle, \tag{56}$$

$$\langle \phi_{\mathrm{f}}^0|\mathbf{T}(E)|\phi_{\mathrm{i}}^0\rangle = \int_0^\infty \mathrm{d}r\, \phi_{\mathrm{f}}^0(r)V(r)\langle r|\Omega^+(E)|\phi_{\mathrm{i}}^0\rangle, \tag{57}$$

$$\langle \phi_{\mathrm{f}}^0|\mathbf{T}(E)|\phi_{\mathrm{i}}^0\rangle = \int_0^\infty \mathrm{d}r\, \phi_{\mathrm{f}}^0(r)V(r)\Psi^+(r;k_{\mathrm{i}},E), \tag{58}$$

where $\Omega^+(E)$ is the Møller operator. The function $\Psi^+(r;k_{\mathrm{i}},E)$ obeys the inhomogeneous Schrödinger equation

$$(E - \mathbf{H})\Psi^+(r;k_{\mathrm{i}},E) = (E - E_{\mathrm{i}})\phi_{\mathrm{i}}^0 \tag{59}$$

and satisfies the boundary condition

$$\Psi^+(r;k_i,E)=0 \quad (r\leqslant a). \tag{60}$$

As r becomes infinite, Ψ^+ behaves as the initial state ϕ_i^0 plus a linear combination of outgoing wave eigenfunctions of $\mathbf{H}_0$ at energy E. Note that beyond the range of the potential such a function will obey Eq. (59). Following Laughlin and Scott [24], we define

$$\begin{aligned}\mathbf{V}\Psi^+(r;k_i,E) &= -(E-E_i)\phi_i^0+\frac{\hbar^2}{2\mu}\frac{d\Psi^+(r;k_i,E)}{dr}\\ &\quad\times\delta(r-a), \quad r\leqslant a,\\ \mathbf{V}\Psi^+(r;k_i,E) &= V(r)\Psi^+(r,k_i,E), \quad r>a.\end{aligned} \tag{61}$$

If only a hard wall were present, the local potential $V(r)$ would be zero for $r>a$.

Now we write Ψ^+ for $r>a$ as

$$\Psi^+(r;k_i,E)=p_i(r)+[\mathbf{G}(E)^+q_i](r), \tag{62}$$

where we define the functions

$$p_{i,f}(r)=c(r)\phi_{i,f}^0 \tag{63}$$

and

$$\begin{aligned}q_{i,f}(r) &= (E-E_{i,f})(1-c(r))\phi_{i,f}^0\\ &\quad-\frac{\hbar^2}{2\mu}\left(2\frac{dc}{dr}\frac{d\phi_{i,f}^0}{dr}+\phi_{i,f}^0\frac{d^2c}{dr^2}\right)\\ &\quad+c(r)V(r)\phi_{i,f}^0.\end{aligned} \tag{64}$$

The regular cutoff function $c(r)$ is defined such that when $r\geqslant r_{max}$, $c(r)=1$ and $dc/dr\approx d^2c/dr^2\approx 0$. Note that with these definitions,

$$(E-\mathbf{H})\Psi^+=(E-E_i)\phi_i^0 \tag{65}$$

for $r>a$, regardless of what $c(r)$ is. Note further that

$$(E-E_{i,f})\phi_{i,f}^0=q_{i,f}+(E-\mathbf{H})p_{i,f}(r). \tag{66}$$

When a hard wall is present, we choose $c(r)$ such that $c(a)=0$. With this choice, $p_i(a)=0$, so that $\chi(a)=[\mathbf{G}^+(E)q_i](a)=0$, and the trial function χ can be expanded in a basis which goes to zero at $r=a$, and likewise with $\tilde{\chi}$.

We now proceed to evaluate the matrix element in Eq. (58). Since $V(r)$ is negligible for $r\geqslant r_{max}=b$, we can truncate the integral in Eq. (58) at $r=b$. We then have

$$\begin{aligned}\langle\phi_f^0|\mathbf{T}(E)|\phi_i^0\rangle &= \int_0^b dr\,\phi_f^0(r)V(r)\Psi^+(r)\\ &= \int_0^a dr\,\phi_f^0(r)V(r)\Psi^+(r)\\ &\quad+\int_a^b dr\,\phi_f^0(r)V(r)\Psi_l(r)\\ &= -(E-E_i)\int_0^a dr\,\phi_f^0(r)\phi_i^0(r)\\ &\quad+\frac{\hbar^2}{2\mu}\phi_f^0(a)\Psi^{+\prime}(a)\\ &\quad+\int_a^b dr\,\phi_f^0(r)V(r)\Psi^+(r),\end{aligned} \tag{67}$$

where the prime denotes differentiation with respect to r. Now we evaluate

$$\begin{aligned}&\int_a^b dr\,\phi_f^0(r)V(r)\Psi^+(r)\\ &\quad=\int_a^b dr\,\phi_f^0(r)(E-H_0)\Psi^+(r)\\ &\qquad-(E-E_i)\int_a^b dr\,\phi_f^0(r)\phi_i^0(r)\\ &\quad=\frac{\hbar^2}{2\mu}\left[\phi_f^0(r)\Psi^{+\prime}(r)-\Psi^+(r)\phi_f^{0\prime}(r)\right]\Big|_a^b\\ &\qquad+(E-E_f)\int_a^b dr\,\phi_f^0(r)\Psi^+(r)\\ &\qquad-(E-E_i)\int_a^b dr\,\phi_f^0(r)\phi_i^0(r)\end{aligned} \tag{68}$$

$$\begin{aligned}&=\frac{\hbar^2}{2\mu}\left[\phi_f^0(b)\Psi^{+\prime}(b)-\Psi^+(b)\phi_f^{0\prime}(b)\right]\\ &\quad-\frac{\hbar^2}{2\mu}\phi_f^0(a)\Psi^{+\prime}(a)+(E-E_f)\\ &\quad\times\int_a^b dr\,\phi_f^0\Psi^+(r).\end{aligned} \tag{69}$$

Evaluating the last integral in Eq. (69), we have

$$(E-E_{\mathrm{f}})\int_a^b \mathrm{d}r\,\phi_{\mathrm{f}}^0(r)\Psi^+(r) \tag{70}$$

$$=\int_a^b \mathrm{d}r\,q_{\mathrm{f}}(r)\Psi^+(r)+\int_a^b \mathrm{d}r\,\Psi^+(r)(E-\mathbf{H})p_{\mathrm{f}}(r) \tag{71}$$

$$=\int_a^b \mathrm{d}r\,q_{\mathrm{f}}(r)\Psi^+(r)+\frac{\hbar^2}{2\mu}\Big[\Psi^+(r)p_{\mathrm{f}}'(r) - p_{\mathrm{f}}(r)\Psi^{+\prime}(r)\Big]\Big|_a^b+\int_a^b \mathrm{d}r\,p_{\mathrm{f}}(r)(E-\mathbf{H})\Psi^+(r) \tag{72}$$

$$=\int_a^b \mathrm{d}r\,q_{\mathrm{f}}(r)\Psi^+(r)+\frac{\hbar^2}{2\mu}\Big[\Psi^+(b)p_{\mathrm{f}}'(b) - p_{\mathrm{f}}(b)\Psi^+(b)'\Big]+\int_a^b \mathrm{d}r\,p_{\mathrm{f}}(r)q_{\mathrm{i}}(r) + \int_a^b \mathrm{d}r\,p_{\mathrm{f}}(r)(E-\mathbf{H})p_{\mathrm{i}}(r) \tag{73}$$

$$=\int_a^b \mathrm{d}r\int_a^b \mathrm{d}r'\,q_{\mathrm{f}}(r)\langle r|\mathbf{G}^+(E)|r'\rangle q_{\mathrm{i}}(r') +\frac{\hbar^2}{2\mu}\Big[\Psi^+(b)p_{\mathrm{f}}'(b)-p_{\mathrm{f}}(b)\Psi^{+\prime}(b)\Big] +\int_a^b \mathrm{d}r\,p_{\mathrm{f}}(r)q_{\mathrm{i}}(r)+\int_a^b \mathrm{d}r\,q_{\mathrm{f}}(r)p_{\mathrm{i}}(r) +\int_a^b \mathrm{d}r\,p_{\mathrm{f}}(r)(E-\mathbf{H})p_{\mathrm{i}}(r). \tag{74}$$

Eq. (71) follows from Eq. (66). Plugging Eq. (74) into Eq. (69) and Eq. (69) into Eq. (67), we get

$$\langle\phi_{\mathrm{f}}^0|V|\Psi^+\rangle=-(E-E_{\mathrm{i}})\int_0^b \mathrm{d}r\,\phi_{\mathrm{i}}^0(r)\phi_{\mathrm{f}}^0(r) +\int_a^b \mathrm{d}r\,q_{\mathrm{f}}(r)[\mathbf{G}(E)^+q_{\mathrm{i}}](r) +\int_a^b \mathrm{d}r\,p_{\mathrm{f}}(r)q_{\mathrm{i}}(r) +\int_a^b \mathrm{d}r\,q_{\mathrm{f}}(r)p_{\mathrm{i}}(r) +\int_a^b \mathrm{d}r\,p_{\mathrm{f}}(r)(E-\mathbf{H})p_{\mathrm{i}}(r). \tag{75}$$

Note that all except the first and last terms in this expression are symmetric with respect to interchange of ϕ_{i}^0 and ϕ_{f}^0. It is a simple exercise to show that the sum of the first and last terms are also symmetric with respect to this interchange (and the simultaneous interchange of E_{i} and E_{f}). Thus, this expression is symmetric, as it should be. Note further that if no hard wall is present ($a=0$) then we can set $c(r)=1$ so that this expression reduces to Eq. (54).

This expression has the advantage over that of Laughlin and Scott (Eq. (23) of Ref. [24], for example) that no local information about $\Psi^+(r)$ is explicitly required; everything is expressed in terms of integrals. Obviously the Green's operator matrix element required is $\langle q_{\mathrm{f}}|\mathbf{G}(E)^+|q_{\mathrm{i}}\rangle$. The other integrals are evaluated by quadrature.

3. Computational details

In the next section we will present off-shell T-matrix calculations for a 1-D Lennard-Jones system considered by Brumer and Shapiro [29] and the model rotationally inelastic H_2–He potential of Johnson and Secrest [35]. In this section, the basis sets and constants used in this paper will be discussed. In all cases $\hbar=1$.

For the 1-D potential, the inhomogeneous Schrödinger equation is

$$\left[E+\frac{\hbar^2}{2\mu}\left(\frac{\mathrm{d}^2}{\mathrm{d}r^2}-\frac{l(l+1)}{r^2}\right) +\epsilon\left[\left(\frac{\sigma}{r}\right)^{12}-\left(\frac{\sigma}{r}\right)^{6}\right]\right]\Psi, \tag{76}$$

$$=(E-E_{\mathrm{i}})j_l(k_{\mathrm{i}}r)/k_{\mathrm{i}}, \tag{77}$$

where $j_l(k_{\mathrm{i}}r)$ is a Ricatti–Bessel function. Due to the singular behavior of the Lennard-Jones potential at $r=0$ we impose hard wall boundary conditions at $r=a>0$. The reduced mass in this paper is 1744.57338 a.u. while ϵ and σ are 5.62×10^{-4} and 5.5 a.u., respectively. These values are the same as those used by Brumer and Shapiro who in turn were studying a model Hg–H_2 scat-

tering problem presented by Marchi and Mueller [36].

The radial coordinate is divided into N sectors of equal length. (The equal size restriction is not necessary, merely convenient.) The ith sector is bounded by radial values r_i and r_{i-1} with $r_0 = a$. On each sector, we make the coordinate transformation

$$x = 2(r - r_{i-1})/(r_i - r_{i-1}) - 1. \tag{78}$$

We then define a discrete variable representation (DVR) based on a suitable function basis (function basis representation (FBR), in the nomenclature of the Light group [37,38]). In the DVR approach, the matrix representation for the coordinate, or a suitable function of the coordinate, evaluated in the FBR is diagonalized,

$$[\mathbf{T}^{\mathrm{T}}\mathbf{x}\mathbf{T}]_{\alpha\beta} = x_\alpha \delta_{\alpha\beta}. \tag{79}$$

The orthogonal matrix $\mathbf{T}$ is the FBR–DVR transformation. In this paper we always diagonalize the coordinate x from Eq. (78). The discrete eigenvalues x_α then yield eigenvalues r_α by means of the inverse transformation. The symmetrized kinetic energy is evaluated in the function basis and transformed to the DVR using $\mathbf{T}$. The potential is approximately diagonal in the DVR,

$$\mathbf{V}^{\mathrm{DVR}}_{\alpha\beta} \approx V(r_\alpha)\delta_{\alpha\beta}. \tag{80}$$

In the studies that appear in this paper, the function basis on the ith sector is always chosen to be classical orthogonal polynomials [39] multiplied by the square roots of their corresponding weight functions, i.e.

$$\phi^i_n(x) = N^i_n w(x)^{1/2} P^i_n(x), \tag{81}$$

where the polynomials P^i_n are orthonormal on the range $x \in (-1, 1)$ with respect to weight $w(x)$ and the normalization coefficient N^i_n makes the functions ϕ_n orthonormal on the range $r \in (r_{i-1}, r_i)$ (with unit weight). With this choice of functions, the transformation matrix has elements [40]

$$\mathbf{T}_{n\alpha} = \sqrt{\omega_\alpha} P^i_n(x_\alpha), \tag{82}$$

where x_α and ω_α are the quadrature points and weights, respectively, of the Gaussian quadrature corresponding to P^i_n. Now, if we wish to evaluate the representation of an $\mathscr{L}^2$ function (on a sector) in the DVR, we begin by expanding it in the FBR,

$$f(x) = \sum_n c_n \phi^i_n(x) \tag{83}$$

and transforming the vector of coefficients c_n to the DVR using the transformation matrix $\mathbf{T}$. Using Eq. (82) and the definition of the functions ϕ^i_n, we can see that the vector $\mathbf{f}$ representing the function $f(x)$ in the DVR has elements

$$\mathbf{f}_\alpha = \omega'_\alpha f(x_\alpha), \tag{84}$$

where $\omega'_\alpha = \omega_\alpha / \sqrt{w(x_\alpha)}$. It is easy to see that if two $\mathscr{L}^2$ functions are represented in this fashion, the inner product of their DVR representations is precisely the inner product of the functions evaluated in the Gaussian quadrature.

For the Lennard-Jones potential problem, we choose on the first sector

$$\phi^1_n = (1 + x)P^{(0,2)}_n, \tag{85}$$

where $P^{(0,2)}_n$ is a Jacobi polynomial [41]. This set of functions, and therefore the corresponding DVR, goes to zero at $r = r_0 = a$, and obeys no fixed boundary conditions at $r = r_1$. For all other sectors, the function basis consists of Legendre functions of x normalized to unity on the range (r_{i-1}, r_i). On each sector except the first, the contribution to each of the integrals in Eq. (75) from that sector is evaluated by the inner product of the DVR representations of the functions $\phi_{\mathrm{i,f}}$, $q_{\mathrm{i,f}}$, $p_{\mathrm{i,f}}$, and so forth. On the first sector, the integral is evaluated via Gauss–Legendre quadrature. The reason for this modification is that except for $p_{i,f}$, the functions appearing in the integrals in Eq. (75) do not go to zero at $r = a$. A Gaussian quadrature based on the Jacobi polynomials $P^{(0,2)}_n$ is not as efficient as a Gauss–Legendre quadrature for such integrals.

If an off-shell T-matrix element is desired at many energies E, it is helpful to diagonalize the energy-independent part of $\tilde{\mathbf{a}}_i$ on each sector; that is, to diagonalize the symmetric part of the

sector Hamiltonian. From Eq. (37), we then see that in the representation of eigenvectors of $\mathbf{H}_i^S$, the matrix $\tilde{\mathbf{a}}_i$ is the sum of a diagonal matrix and a low-rank nondiagonal matrix, since the dimension of $\mathbf{U}_l^i$ is $n_i \times 2$ with $n_i \gg 2$. Thus, this matrix is inverted very easily by means of the Sherman–Woodbury formula [42]. The matrices $\mathbf{U}_l^i$ and $\mathbf{U}_r^i$ and the vectors $\mathbf{f}_i$ and $\mathbf{g}_i$ must also be transformed into the eigenvector basis to evaluate the Green's operator matrix element correctly, of course.

This paragraph assumes that the original basis is orthogonal, which is always the case in this paper.

For the rotationally inelastic H_2–He model, we choose as a coordinate system the spherical polar coordinates in a space-fixed frame of the vector $\mathbf{r}$ between the H atoms and the vector $\mathbf{R}$ from the H_2 center of mass to the He atom. The magnitude of $\mathbf{r}$ is fixed at r_0 ($=1$ a.u. in this paper), so the coordinate space is 5-D. The scattering coordinate is R, the magnitude of $\mathbf{R}$. As in the 1-D problem, R is divided into N sectors of equal size. On each sector i a basis is constructed of the form

$$\Phi_{nlj}^{iJM} = \phi_{nl}(R)\mathscr{Y}_{jl}^{JM}(\hat{\mathbf{r}}, \hat{\mathbf{R}}), \tag{86}$$

where $\hat{\mathbf{r}}$ and $\hat{\mathbf{R}}$ are the unit vectors along $\mathbf{r}$ and $\mathbf{R}$, respectively, and

$$\mathscr{Y}_{jl}^{JM} = \sum_{m_l, m_j} \langle jm_j lm_l | JM \rangle Y_{jm_j}(\hat{\mathbf{r}}) Y_{lm_l}(\hat{\mathbf{R}}), \tag{87}$$

where $\langle jm_j lm_l | JM \rangle$ is a Clebsch–Gordan coefficient [43]. The inhomogeneous Schrödinger equation then has the form

$$\left[E + \frac{\hbar^2}{2\mu_1}\nabla_{\mathbf{R}}^2 + \frac{\hbar^2}{2\mu_2}\nabla_{\mathbf{r}}^2 - V(R, \hat{\mathbf{r}}\cdot\hat{\mathbf{R}})\right]\Psi = (E - E_i) j_{l_i}(k_i R)\mathscr{Y}_{l_i j_i}^{JM}/k_i. \tag{88}$$

The reduced masses are $\mu_1 = m_{He}m_{H_2}/(m_{He} + m_{H_2}) = 2448.909$ a.u. and $\mu_2 = m_{H_2}/2 = 1799.381$ a.u.

Following common practice [35,43], we expand the potential in a Legendre series in the angle between $\mathbf{R}$ and $\mathbf{r}$,

$$V(R, \hat{\mathbf{R}}\cdot\hat{\mathbf{r}}) = \sum_\lambda V_\lambda(R) P_\lambda(\hat{\mathbf{R}}\cdot\hat{\mathbf{r}}). \tag{89}$$

On sectors with $i > 1$, the radial factor of the basis is a Legendre DVR in $x = 2(R - R_{i-1})/(R_i - R_{i-1}) - 1$, as in the 1-D case. On these sectors, then, the potential is (approximately) diagonal in the radial factor, as in the 1-D case

$$V_{jl\alpha;j'l'\beta}^{JM} = \delta_{\alpha\beta}\sum_\lambda V_\lambda(R(x_\alpha)) f_{j'l'jl\lambda}^{JM}, \tag{90}$$

where

$$f_{j'l'jl\lambda}^{JM} = \int d\hat{\mathbf{r}} \int d\hat{\mathbf{R}} \mathscr{Y}_{j'l'}^{JM*}(\hat{\mathbf{R}}, \hat{\mathbf{r}}) P_\lambda(\hat{\mathbf{R}}\cdot\hat{\mathbf{r}}) \mathscr{Y}_{jl}^{JM}(\hat{\mathbf{R}}, \hat{\mathbf{r}}), \tag{91}$$

the formula for which is given in Eq. (44) of Ref. [43]. For the Johnson–Secrest potential [35], the Legendre coefficients are given by

$$V_0(r) = V_0 e^{-\alpha r},$$
$$V_2(r) = \beta V_0 e^{-\alpha r},$$
$$V_{i\neq 0,2} = 0$$

with $V_0 = 17.2828$ a.u., $\alpha = 2.027$ a.u. and $\beta = 0.375$.

If we add a hard wall to the potential at $R = a > 0$, then we can also choose a radial basis consisting of a Jacobi DVR based on the polynomials $P_n^{(0,2)}$, as in the 1-D case, and once again the potential will be diagonal in the DVR. When the potential is nonsingular so that the origin is physically accessible, it may be more appropriate to choose a radial basis which depends on the orbital angular momentum l. We choose a DVR based on Jacobi functions of order $(0, 2l)$,

$$\phi_{nl} = N_n^l (1 + x)^l P_n^{(0,2l)}(x). \tag{92}$$

These functions behave as R^l as $R \to 0$ because of the weight function. Potential matrix elements corresponding to $l = l'$ will still be diagonal in the radial factor of the resulting basis. Since different l values give rise to different DVR's, the potential

couples different DVR points when $l \neq l'$. To compute such matrix elements, we first compute the overlaps of the Jacobi functions for different l's,

$$\mathbf{O}^{ll'}_{nn'} = N^l_n N^{l'}_{n'} \int \mathrm{d}x (1+x)^{l+l'} P^{(0,2l)}_n(x) P^{(0,2l')}_{n'}(x). \tag{93}$$

These matrix elements can be computed exactly using the recursion relations among different Jacobi polynomials [41]. Labeling the DVR–FBR transformation matrix for orbital angular momentum l as $\mathbf{T}^l$, we have for $l > l'$

$$V^{JM}_{jl\alpha;j'l'\beta} = \sum_{\lambda nn'} \mathbf{T}^l_{n\alpha} \mathbf{O}^{ll'}_{nn'} \mathbf{T}^{l'}_{n'\beta} V_\lambda\left(R\left(x^{l'}_\beta\right)\right) f^{JM}_{j'l'jl\lambda}. \tag{94}$$

Since total angular momentum is conserved in this problem, all matrices are diagonal in J. To complete the description of the basis, we must choose which functions $\mathscr{Y}^{JM}_{lj}$ to include on each sector; that is, which values of l and j to include in the basis for fixed J. (All matrix elements in this problem are independent of M, which is set to zero.) Recall that the functions $\mathscr{Y}^{JM}_{lj}$ are eigenfunctions of the parity operator with eigenvalues $(-1)^{l+j}$ [43]. We then choose a maximum number of rotor states n_j independent of the sector. For an accurate description of the matrix elements, this set may have to include some rotor quantum numbers corresponding to channels that are closed at energy E [33]. Then all orbital angular momenta l consistent with the triangle inequality $|J-j| \leqslant l \leqslant J+j$ and parity constraints are included in the basis.

To define the surface basis used to impose the constraints of continuity and differentiability with respect to R at the sector boundaries, the surface Hamiltonian at each boundary value $R = R_i$ was computed in the basis $\mathscr{Y}^{JM}_{lj}$ and diagonalized. The surface Hamiltonian eigenvectors were used as the surface basis.

The kinetic energy operators are diagonal in the functions $\mathscr{Y}^{JM}_{lj}$; thus, to compute the kinetic energy matrix elements, we evaluate the radial derivative operators in the radial function bases and transform them to the DVR using the FBR–DVR transformation matrices just as in the 1-D case. Likewise, when evaluating the components of an $\mathscr{L}^2$ function in our basis, each angular momentum component of the function is evaluated in the radial DVR as in the 1-D case.

4. Results

In this section we examine the off-shell T-matrix as a function of initial and final wavenumber k_i and k_f, respectively, for the models discussed in the previous section. Fig. 1 shows the off-shell T-matrix at energy $E = 0.0018375$ a.u. and $j = 0$ for the Lennard-Jones potential. The hard wall is fixed at $r_0 = 2$ a.u and $r_{\max} = 105$ a.u. For initial and final energies less than E the T-matrix exhibits a complicated oscillatory structure. As k_i and k_f approach $k_E = \sqrt{2\mu E}/\hbar$ the width of the variation

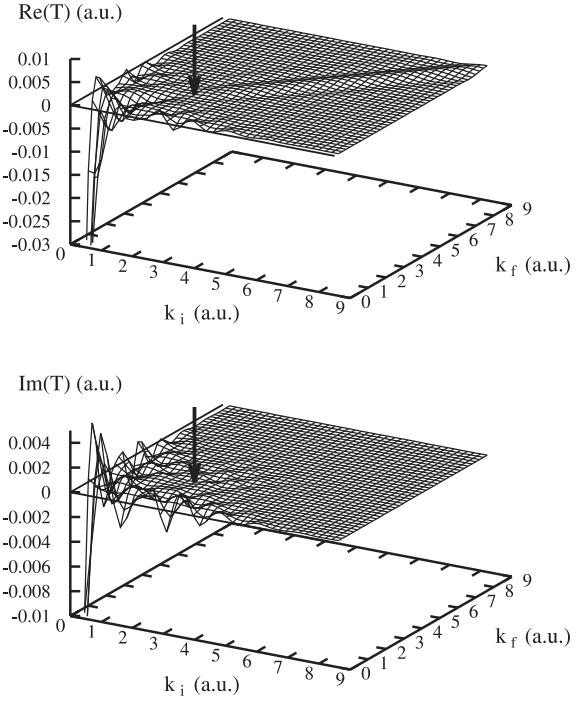

Fig. 1. Real and imaginary parts of the T-matrix for the 1-D Lennard-Jones potential as functions of initial and final asymptotic momenta k_i and k_f, respectively, for $E = 0.0018375$ a.u. and $j = 0$. The arrows point to the on-shell values.

about the line $k_i = k_f$ decreases. When k_i and k_f are larger than k_E, the imaginary part of the T-matrix goes to zero while the real part has a narrow ridge along the line $k_i = k_f$. This ridge does not decay in magnitude but approaches, for $k_i = k_f$, a constant value of $\hbar^2 r_0/4\mu = 2.866 \times 10^{-4}$ a.u. This approach to a constant value is a manifestation of the hard wall. This result also appears in the paper of Laughlin and Scott [24] for hard-wall scattering (corrected for differences in units and normalization).

Fig. 2 shows the T-matrix for $j = 12$. Once again there is a low-energy region characterized by complicated structure in the T-matrix and a high-energy region characterized by a ridge in the real part of the T-matrix that changes very little along the line $k_i = k_f$ and rapid decays to zero as $|k_i - k_f|$ becomes large. Unlike the $j = 0$ case, the two regions overlap. The amplitude of this T-matrix is two orders of magnitude less than that for the $j = 0$ case, a result consistent with those of Brumer and Shapiro for the same potential [29] which indicates the convergence of the partial wave expansion for the T-matrix. Note that the symmetry in the T-matrix elements with respect to interchange of k_i and k_f, which is not obvious from Eq. (75), is apparent in this plot. The on-shell values of the T-matrix obviously appear on the line $k_i = k_f$. The T-matrix along this line, with the on-shell values, is shown in Fig. 3.

To assess the convergence properties of this method – and to substantiate the claim that the results shown so far are indeed off-shell T-matrix elements – we test the off-shell unitarity of the results shown in Fig. 1. One version of the off-shell unitarity relation for a T-matrix element, given our choice of normalization is [44]

$$\mathrm{Im}(t_{kk'}(E)) = -2\mu k_E t_{kk_E}(E)^* t_{k'k_E}(E), \tag{95}$$

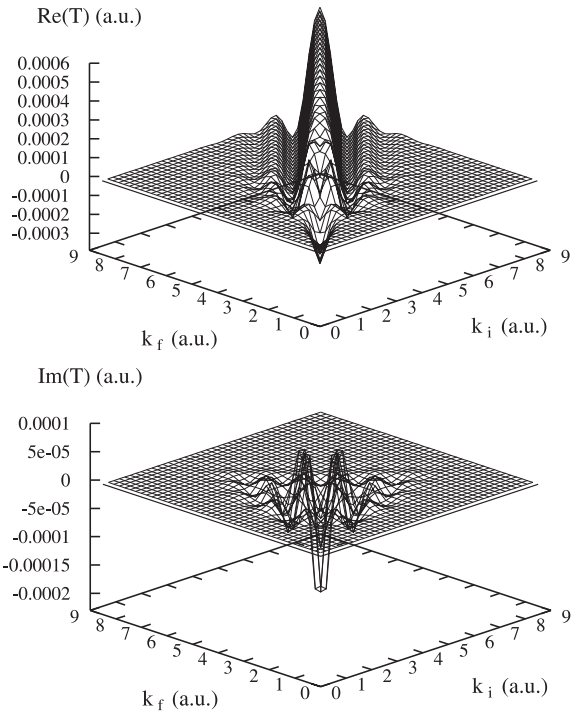

Fig. 2. Real and imaginary parts of the T-matrix for the 1-D Lennard-Jones potential as functions of initial and final asymptotic momenta k_i and k_f, respectively, for $E = 0.0018375$ a.u. and $j = 12$.

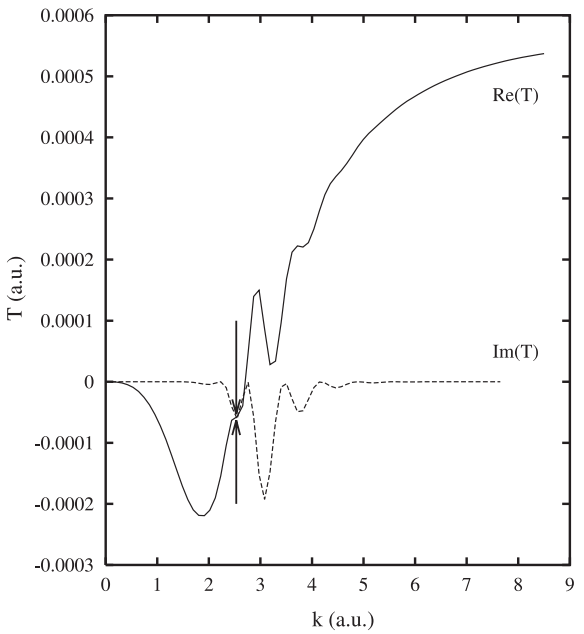

Fig. 3. Real and imaginary parts of the T-matrix for the 1-D Lennard-Jones potential from Fig. 2 along the line $k_i = k_f = k$. The arrows point to the on-shell values.

where $k_E = \sqrt{2\mu E}/\hbar$ and $t_{kk'}(E) = \langle k|T(E)|k'\rangle$. The results plotted in Fig. 1 are the T-matrix plotted on a uniform 40×40 grid of initial and final wavenumbers. We define a maximum error $\Delta_{\max}$ by

$$\Delta_{\max} = \max_{\text{grid}} \left\{ [\mathrm{Im}(t_{kk'}(E)) + 2\mu k_E t_{kk_E}(E)^* t_{k'k_E}(E)]/ \min(|\mathrm{Im}(t_{kk'}(E))|, |2\mu k_E t_{kk_E}(E)^* t_{k'k_{\mathrm{II}}}(E)|) \right\}, \tag{96}$$

the largest relative difference between the two sides of Eq. (95) among all the T-matrix values on the grid. The maximum error as a function of number of sectors N and the number of basis functions n per sector is shown in Table 1. We can see that keeping the number of sectors fixed and increasing the number of basis functions per sector leads to more rapid convergence than keeping n fixed and increasing N. This behavior is typical of a finite element calculation of this type [45].

Fig. 4 shows the T-matrix for the model H_2–He potential for $J = j_i = j_f = l_i = l_f = 0$ and energy $E = 1.8375 \times 10^{-3}$ a.u. The radial range was truncated at $R = 15$ a.u. The structure is quite similar to the $j = 0$ T-matrix for the Lennard-Jones potential. The ridge in this case gradually decays to zero. Fig. 5 shows the same T-matrix at the higher energy $E = 8.3326 \times 10^{-3}$ a.u. The "low-energy" region of complicated oscillations is substantially larger than in Fig. 4, and the peaks in both the real and imaginary parts of the T-matrix have a larger amplitude. The high-energy ridge is still present but is too small to be seen on the scale of the low-energy peaks.

Table 1
Maximum deviation $\Delta_{\max}$ from off-shell unitarity of the results from Fig. 1 as a function of radial basis n per sector and the number of sectors N

n	N	$\Delta_{\max}$
5	320	4.5×10^{-4}
7	320	1.3×10^{-7}
9	320	4.6×10^{-8}
11	320	1.9×10^{-8}
5	360	4.5×10^{-4}
5	400	2.2×10^{-4}
5	450	7.0×10^{-5}
5	500	2.0×10^{-5}

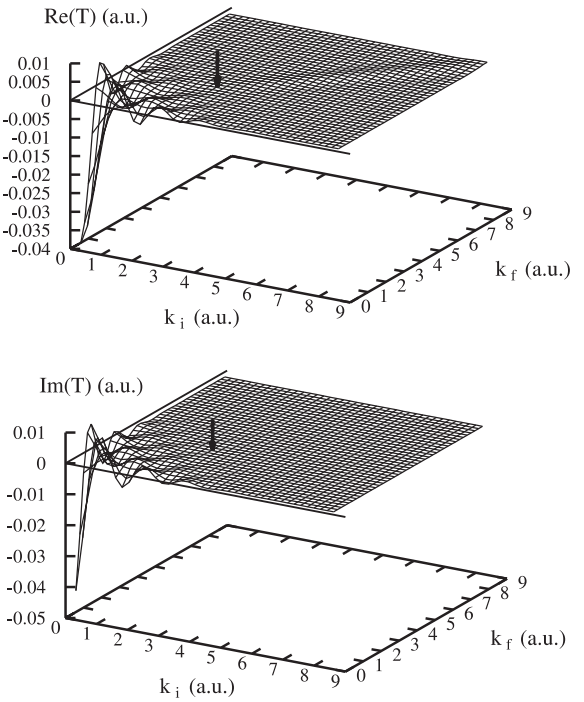

Fig. 4. Real and imaginary parts of the T-matrix for the model H_2–He problem as functions of initial and final asymptotic momenta k_i and k_f, respectively, for $E = 0.0018375$ a.u., total angular momentum $J = 0$, initial orbital and rotor angular quantum numbers $l_i = 0$ and $j_i = 0$, respectively, and final orbital and rotor angular quantum numbers $l_f = 0$ and $j_f = 0$, respectively. The arrows point to the on-shell values.

Fig. 6 shows the T-matrix for $J = 6$, $j_i = j_f = 2$, $l_i = 8$, $l_f = 4$, and $E = 1.8375 \times 10^{-3}$ a.u. The structure present at the origin in the $J = 0$ plots is suppressed by the centrifugal potential (an effect seen in the $l = 12$ T-matrix for the 1-D potential as well). The high-energy ridge is also present but there is more oscillation along the lines perpendicular to $k_i = k_f$ than in the elastic transitions shown in Figs. 4 and 5.

Fig. 7 shows the T-matrix for $J = 17$, $j_i = 0$, $j_f = 2$, $l_i = l_f = 17$, and $E = 1.8375 \times 10^{-3}$ a.u. The on-shell values are essentially zero, consistent with a rapid convergence of the partial wave expansion of the scattering wavefunction. While the low energy oscillatory region is present, the real part is dominated by the high-energy ridge.

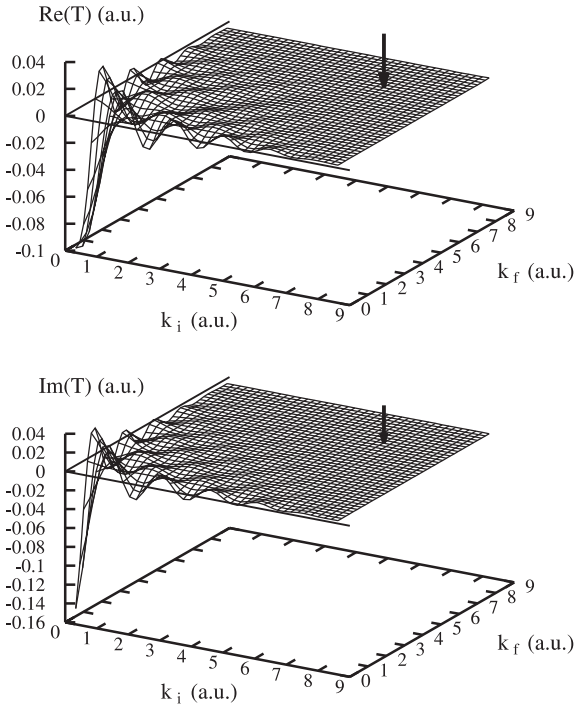

Fig. 5. Real and imaginary parts of the T-matrix for the model H_2–He problem as functions of initial and final asymptotic momenta k_i and k_f, respectively, for $E = 0.0083362$ a.u., total angular momentum $J = 0$, initial orbital and rotor angular quantum numbers $l_i = 0$ and $j_i = 0$, respectively, and final orbital and rotor angular quantum numbers $l_f = 0$ and $j_f = 0$, respectively. The arrows point to the on-shell values.

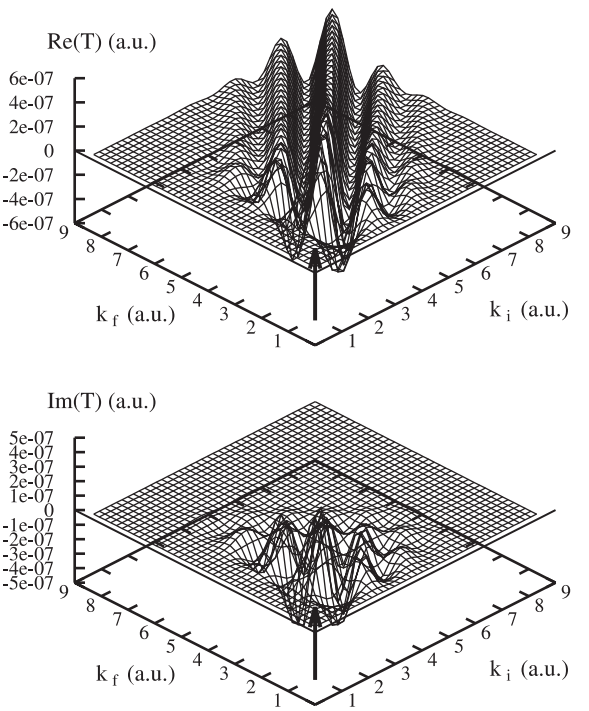

Fig. 6. Real and imaginary parts of the T-matrix for the model H_2–He problem as functions of initial and final asymptotic momenta k_i and k_f, respectively, for $E = 0.0018375$ a.u., total angular momentum $J = 6$, initial orbital and rotor angular quantum numbers $l_i = 8$ and $j_i = 2$, respectively, and final orbital and rotor angular quantum numbers $l_f = 4$ and $j_f = 2$, respectively. The arrows point to the on-shell values.

All the results for both model systems share a number of characteristics: a low-energy region characterized by highly oscillatory variations in the T-matrix that depend strongly on energy and angular momentum; a high-energy ridge that decays very slowly to a constant value (zero if no hard wall is present) as k_i and k_f become large, which oscillates along lines of constant $k_i + k_f$ to a degree that depends on whether the transition is inelastic or not, and which depends relatively weakly on energy. How general these properties are remains to be seen.

5. Conclusion

I have presented a cellular variant of the Kohn variational algorithm for the Green's operator which admits a recursive computation of its matrix elements. The technique presented is essentially a rearrangement of the equations that result from the variational formula of Miller and Jansen op de Haar [33] within a finite element basis [46]. In addition, a convenient expression for off-shell T-matrix elements has been derived which is be applicable even when the potential has a hard wall component, and which is amenable to computation via the recursive KVP. The technique appears to be stable and rapidly convergent on the test cases presented herein.

It should also be stressed that *any* matrix element of a Green's operator can be computed using the present recursive algorithm, provided that the potential is local.

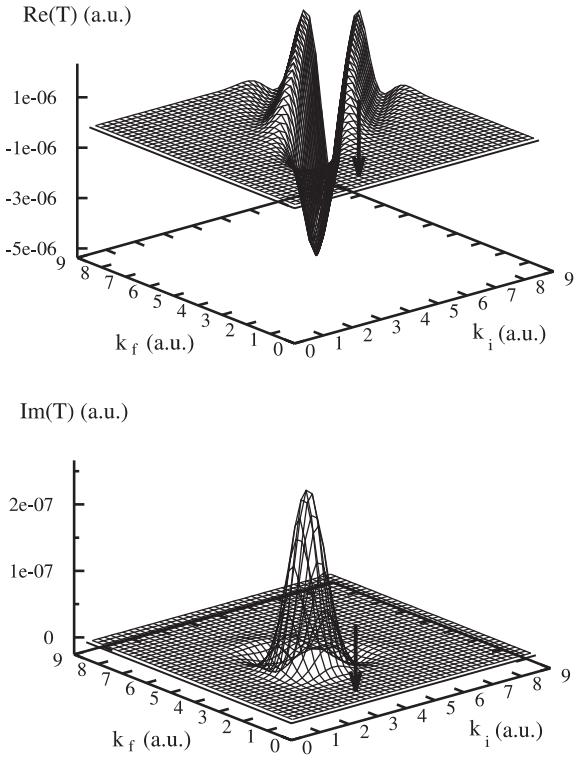

Fig. 7. Real and imaginary parts of the T-matrix for the model H_2–He problem as functions of initial and final asymptotic momenta k_i and k_f, respectively, for $E = 0.0018375$ a.u., total angular momentum $J = 17$, initial orbital and rotor angular quantum numbers $l_i = 17$ and $j_i = 0$, respectively, and final orbital and rotor angular quantum numbers $l_f = 17$ and $j_f = 2$, respectively. The arrows point to the on-shell values.

Acknowledgements

This work was funded by the Astrophysics Division, NASA Office of Space Science, and by the Environmental Sciences Division of the United States Department of Energy Atmospheric Radiation Measurement Program under grant ER-16774. I would like to express my gratitude to the late Sheldon Green for suggesting this work.

References

[1] J.R. Taylor, Scattering Theory: The Quantum Theory of Nonrelativistic Collisions, Krieger, Malabar, 1983.
[2] N.M. Kroll, K.M. Watson, Phys. Rev. A 8 (1973) 804.
[3] B. Wallbank, J.K. Holmes, Phys. Rev. A 48 (1993) R2515.
[4] B. Wallbank, J.K. Holmes, J. Phys. B 27 (1994) 5405.
[5] B. Wallbank, J.K. Holmes, J. Phys. B 29 (1996) 5881.
[6] D.B. Milošević, J. Phys. B 28 (1995) 1869.
[7] A. Jaroń, J.Z. Kamiński, Laser Phys. 9 (1998) 81.
[8] M. Baranger, Phys. Rev. 111 (1958) 481.
[9] U. Fano, Phys. Rev. 131 (1963) 259.
[10] A. Ben-Reuven, Phys. Rev. 145 (1966) 7.
[11] C.D. Ball, M. Mengel, F.C. De Lucia, D.E. Woon, J. Chem. Phys. 111 (1999) 8893.
[12] C. Quigg, C.J. Joachain, Rev. Mod. Phys. 46 (1974) 279.
[13] G. Chew, Phys. Rev. 80 (1950) 196.
[14] R.D. Sharma, P.M. Bakshi, J.M. Sindoni, Phys. Rev. A 43 (1991) 189.
[15] H. Cheng, K. Yang, E. Vilallonga, H. Rabitz, Phys. Rev. A 49 (1994) 1096.
[16] R. Elber, R.B. Gerber, D.J. Kouri, Chem. Phys. 97 (1985) 345.
[17] E.O. Alt, A.S. Kadyrov, A.M. Mukhamedzhanov, Phys. Rev. A 60 (1999) 314.
[18] M. Shugard, A.U. Hazi, Phys. Rev. A 12 (1975) 1895.
[19] M.A. Morrison, J. Phys. B 19 (1986) L707.
[20] J.M.J. van Leeuwen, A.S. Reiner, Physica 27 (1961) 99.
[21] K.L. Kowalski, D. Feldman, J. Math. Phys. 2 (1961) 499.
[22] K.L. Kowalski, D. Feldman, J. Math. Phys. 4 (1963) 507.
[23] D.Y. Wong, G. Zambotti, Phys. Rev. 154 (1967) 1540.
[24] R. Laughlin, B.L. Scott, Phys. Rev. 171 (1968) 1196.
[25] G.L. Payne, J.D. Perez, Phys. Rev. C 10 (1974) 1584.
[26] D.J. Kouri, F.S. Levin, Phys. Rev. C 10 (1974) 2096.
[27] B. Talukdar, M.N. Sinha Roy, N. Mallick, D.K. Nayek, Phys. Rev. C 12 (1975) 370.
[28] P. Eckelt, H.J. Korsch, V. Philipp, J. Phys. B 7 (1974) 1649.
[29] P. Brumer, M. Shapiro, J. Chem. Phys. 63 (1975) 427.
[30] R.B. Gerber, Mol. Phys. 42 (1980) 693.
[31] H. Cheng, E. Vilallonga, H. Rabitz, Phys. Rev. A 42 (1990) 5232.
[32] S.K. Adhikari, Variational Principles and the Numerical Solution of Scattering Problems, Wiley, New York, 1998.
[33] W.H. Miller, B.M.D.D. Jansen op de Haar, J. Chem. Phys. 86 (1987) 6213.
[34] R.K. Nesbet, Variational Methods in Electron–Atom Scattering Theory, Plenum Press, New York, 1980.
[35] B.R. Johnson, D. Secrest, J. Chem. Phys. 48 (1968) 4682.
[36] R.P. Marchi, C.R. Mueller, J. Chem. Phys. 38 (1964) 740.
[37] J.C. Light, I.P. Hamilton, J.V. Lill, J. Chem. Phys. 82 (1985) 1400.
[38] Z. Bačić, J.C. Light, Ann. Rev. Phys. Chem. 40 (1989) 469.
[39] A.F. Nikiforov, S.K. Suslov, V.B. Uvarov, Classical Orthogonal Polynomials of a Discrete Variable, Springer, Berlin, 1991.
[40] A.S. Dickinson, P.R. Certain, J. Chem. Phys. 49 (1968) 4902.
[41] M. Abramowitz, I.A. Stegun, Handbook of Mathematical Functions, Dover, New York, 1965.
[42] W.H. Press, S.A. Teukolsky, W.P. Vetterling, B.P. Flannery, Numerical Recipes, second ed., Cambridge University Press, Cambridge, 1992.

[43] A.M. Arthurs, A. Dalgarno, Proc. R. Soc. Lond A 256 (1960) 540.
[44] K.M. Watson, J. Nutall, Topics in Several Particle Dynamics, Holden-Day, CA, 1967.
[45] I. Babuska, B. Szabo, Int. J. Num. Meth. Engng. 18 (1982) 323.
[46] D. Zwillinger, Handbook of Differential Equations, Academic Press, Boston, 1989, p. 553.